HHS Public Access

Author manuscript

Sci Transl Med. Author manuscript; available in PMC 2015 July 14.

Published in final edited form as:

Sci Transl Med. 2014 May 28; 6(238): 238ra71. doi:10.1126/scitranslmed.3008004.

Hematopoietic Stem Cell Origin of *BRAF*V600E Mutations in Hairy Cell Leukemia

Stephen S. Chung[#1,2], **Eunhee Kim**[#1], **Jae H. Park**[#2], **Young Rock Chung**[1], **Piro Lito**[3], **Julie Teruya-Feldstein**[4], **Wenhuo Hu**[1], **Wendy Beguelin**[5], **Sebastien Monette**[6], **Cihangir Duy**[5], **Raajit Rampal**[1,2], **Leon Telis**[1], **Minal Patel**[1], **Min Kyung Kim**[1], **Kety Huberman**[7], **Nancy Bouvier**[1,4,7], **Michael F. Berger**[1,4,7], **Ari M. Melnick**[5], **Neal Rosen**[3], **Martin S. Tallman**[2], **Christopher Y. Park**[#1,4,8,9,†], and **Omar Abdel-Wahab**[#1,2,†]

[1]Human Oncology and Pathogenesis Program, Memorial Sloan Kettering Cancer Center, New York, NY 10065, USA

[2]Leukemia Service, Department of Medicine, Memorial Sloan Kettering Cancer Center, New York, NY 10065, USA

[3]Molecular Pharmacology and Chemistry, Memorial Sloan Kettering Cancer Center, New York, NY 10065, USA

[4]Department of Pathology, Memorial Sloan Kettering Cancer Center, New York, NY 10065, USA

[5]Division of Hematology/Oncology, Department of Medicine, Weill Cornell Medical College, New York, NY 10021, USA

[6]Tri-Institutional Laboratory of Comparative Pathology, Memorial Sloan Kettering Cancer Center, Weill Cornell Medical College, Rockefeller University, New York, NY 10065, USA

[7]Center for Molecular Oncology, Memorial Sloan Kettering Cancer Center, New York, NY 10065, USA

[†]Corresponding author. parkc@mskcc.org (C.Y.P.); abdelwao@mskcc.org (O.A.-W.).

SUPPLEMENTARY MATERIALS

www.sciencetranslationalmedicine.org/cgi/content/full/6/238/238ra71/DC1

Materials and Methods

Fig. S1. HSPC abnormalities in HCL and the presence of *BRAF*V600E in HSCs.

Fig. S2. Effect of *BRaf*V600E expression at different time points and stages of hematopoiesis.

Fig. S3. Effect of *BRaf*V600E expression on fetal hematopoiesis and in mice with B cell–restricted expression of the mutant allele.

Fig. S4. Effect of *BRaf*V600E expression on HSPC numbers and frequencies.

Fig. S5. Effect of *BRaf*V600E expression on B cell development and self-renewal.

Fig. S6. Normalization of HSPC compartment and increased myeloid/erythroid output from *BRAF*V600E-mutant HSPCs after BRAF inhibition.

Table S1. Genotyping results of cell populations sorted from HCL patient BM aspirates.

Table S2. Three hundred genes sequenced in three HCL leukemic cell and granulocyte genomic DNA samples.

Author contributions: S.S.C., E.K., J.H.P., M.S.T., C.Y.P., and O.A.-W. designed the study. S.S.C., C.Y.P., W.H., and O.A.-W. performed sorting of human samples. E.K., L.T., Y.R.C., and M.K.K. helped with animal generation, genotyping, and maintenance, as well as experiments involving animals. P.L. and N.R. provided PLX4720 and assistance and advice with drug studies. W.B., C.D., and A.M.M. helped with GC studies and immunohistochemistry. J.T.-F., S.M., and C.Y.P. performed phenotypic and histologic analysis of tissues. J.H.P., R.R., M.P., and M.S.T. helped with collection of patient materials for study. K.H., N.B., and M.F.B. performed genetic analyses on sorted cell populations. S.S.C., E.K., Y.R.C., and O.A.-W. analyzed the data. S.S.C., E.K., and O.A.-W. prepared the manuscript with input from the other authors.

Competing interests: A.M.M. serves as a consultant for Celgene, is part of the speaker bureau for Genentech Basic Science Education Program, and is on the scientific advisory board for Bio-Reference Laboratories. The other authors declare that they have no competing interests.

[8]Department of Laboratory Medicine, Memorial Sloan Kettering Cancer Center, New York, NY 10065, USA

[9]Cell and Developmental Biology, Weill Cornell Medical College, New York, NY 10065, USA

[#] These authors contributed equally to this work.

Abstract

Hairy cell leukemia (HCL) is a chronic lymphoproliferative disorder characterized by somatic *BRAF*V600E mutations. The malignant cell in HCL has immunophenotypic features of a mature B cell, but no normal counterpart along the continuum of developing B lymphocytes has been delineated as the cell of origin. We find that the *BRAF*V600E mutation is present in hematopoietic stem cells (HSCs) in HCL patients, and that these patients exhibit marked alterations in hematopoietic stem/progenitor cell (HSPC) frequencies. Quantitative sequencing analysis revealed a mean *BRAF*V600E-mutant allele frequency of 4.97% in HSCs from HCL patients. Moreover, transplantation of *BRAF*V600E-mutant HSCs from an HCL patient into immunodeficient mice resulted in stable engraftment of *BRAF*V600E-mutant human hematopoietic cells, revealing the functional self-renewal capacity of HCL HSCs. Consistent with the human genetic data, expression of *BRaf*V600E in murine HSPCs resulted in a lethal hematopoietic disorder characterized by splenomegaly, anemia, thrombocytopenia, increased circulating soluble CD25, and increased clonogenic capacity of B lineage cells—all classic features of human HCL. In contrast, restricting expression of *BRaf*V600E to the mature B cell compartment did not result in disease. Treatment of HCL patients with vemurafenib, an inhibitor of mutated BRAF, resulted in normalization of HSPC frequencies and increased myeloid and erythroid output from HSPCs. These findings link the pathogenesis of HCL to somatic mutations that arise in HSPCs and further suggest that chronic lymphoid malignancies may be initiated by aberrant HSCs.

INTRODUCTION

Hairy cell leukemia (HCL) is a chronic lymphoproliferative disorder characterized as a mature B cell malignancy based on the fact that the hallmark leukemic cell in HCL expresses CD19, surface immunoglobulin (1), and clonal rearrangements of immunoglobulin heavy and light chain genes (2, 3)—all features of mature B cells (4, 5). At the same time, HCL cells also express cell surface markers not present on normal B cells, including CD103 and CD11c, antigens typically expressed on intraepithelial T cells and monocytes, respectively (6, 7). In addition, HCL patients have long been known to have clinical features disparate from most mature B cell malignancies, including the absence of lymph node involvement and frequent splenomegaly due to extramedullary hematopoiesis (EMH) (4). Gene expression microarray studies have not precisely identified a specific B cell population as the cell of origin of HCL (8). Hence, the hematopoietic population that initiates and propagates HCL has not been definitively delineated, and the cell of origin of HCL has remained under debate (9-12).

Tiacci *et al.* recently identified somatic *BRAFV*600E mutations in nearly 100% of classic HCL patients (13), a finding since confirmed in multiple studies (14, 15). This seminal observation provided the first genetic insight into HCL pathogenesis and a clonal marker to

track the origin and propagation of HCL. We therefore sought to identify the cell of origin of HCL by identifying the point of hematopoietic development at which the *BRAFV*600E mutation arises.

Here, we identify the presence of the *BRAFV*600E mutation in hematopoietic stem cells (HSCs) in patients with HCL, as well as consistent abnormalities in hematopoietic stem and progenitor cell (HSPC) frequencies in HCL patients. We also use murine genetic models to functionally characterize the effects of mutant *BRaf*V600E expression at various stages of development and hematopoietic differentiation, revealing that many of the characteristic clinical features of HCL are seen only with expression of *BRaf*V600E in cells less mature than committed B cells. Finally, we evaluated the effect of mutant *BRAF* inhibition on hematopoiesis in our murine models, as well as in patients with *BRAF*-mutant HCL using material from patients in an ongoing clinical trial of vemurafenib for relapsed/refractory HCL.

RESULTS

Altered HSPC composition and the presence of *BRAF*V600E mutations in HSCs from HCL patients

To identify the cell population along the hematopoietic hierarchy in which the *BRAF*V600E mutation arises, we prospectively purified HSCs [lineage-negative (LN) $CD34^+$ $CD38^-$ $CD90^+$ $CD45RA^-$], pro-B cells (LN $CD34^+$ $CD38^+$ $CD10^+$ $CD19^+$), hematogones ($CD34^-$ $CD38^{++}$ $CD10^+$ $CD19^+$), myeloid progenitor (MP) cells (LN $CD10^-$ $CD19^-$ $CD34^+$ $CD38^+$ $CD45RA^{+/-}$ $CD123^{+/-}$), and HCL cells ($CD19^+$ $CD103^+$ $CD11c^+$) from the bone marrow (BM) of 14 HCL patients and age-matched controls (Fig. 1A and table S1). CD10, CD19, CD103, and CD11c were excluded from the lineage cocktail and stained with different fluorochromes to assess B and HCL cell frequencies. HCL patients were characterized by an expansion of HSCs among $CD34^+$ $CD38^-$ LN cells and a marked decrease in the frequency of granulocyte-macrophage progenitor (GMP) cells among MPs, consistent with the neutropenia and monocytopenia characteristic of HCL (Fig. 1B). This stage-specific dropout of GMPs was also linked to a decrease in the lymphoid-primed multipotent progenitor population (LMPP; LN $CD34^+$ $CD38^-$ $CD90^-$ $CD45RA^+$) (Fig. 1B), which has been shown to have granulocyte/macrophage-restricted myeloid, as well as normal lymphoid differentiation potential (16, 17). We then used an allele-specific oligonucleotide assay to assess for the *BRAF*V600E mutation (14) in different hematopoietic subsets after double FACS (fluorescence-activated cell sorting) to ensure >97% purity (fig. S1). We identified the *BRAF*V600E mutation in the HSC, pro-B cell, and HCL cell populations of HCL patients (Fig. 1, C and D). Analysis of sorted chronic lymphocytic leukemia (CLL) cells in addition to HCL cells from one individual harboring both diseases identified the presence of the *BRAF*V600E mutation in both cell populations, suggesting a potential shared origin of these two leukemias (Fig. 1E). These data suggest that HCL initiates within the HSPC compartment and not in committed lymphoid cells as previously suggested (9-12).

Genetic and functional evaluation of HSPCs in HCL

Next, to more quantitatively define the proportion of HSCs bearing mutant *BRAF* in HCL patients, we performed quantitative sequencing of the region of *BRAF*V600E in complementary DNA (cDNA) from prospectively purified HCL cells, hematogones, and HSCs (LN $CD34^+$ $CD38^-$ $CD90^+$ $CD45RA^-$) from five different HCL patients. At a mean sequencing depth of >1000×, we identified a mean variant allele frequency (VAF) of 63.1% (+12.1%), 23.0% (+22.9%), and 4.97% (±1.9%) in HCL cells, hematogones, and HSCs, respectively (Fig. 2A). The variability of the *BRAF*V600E VAF in HCL cells was due to the fact that two of the five patients had a homozygous *BRAF*V600E mutation, whereas the others had a heterozygous mutation. In contrast to the mean VAF of >1% in HCL cells, hematogones, and HSCs, the *BRAF*V600E mutation was detected at a VAF of only 0.09% (±0.03%) and 0.07% (±0.009%) in MP and $CD14^+$ cells, respectively (table S1).

Given the high frequency of *BRAF*V600E mutations in HCL and the fact that the mutation was identified in HSCs, we sought to identify additional co-occurring genetic lesions along the course of hematopoietic differentiation that might cooperate with the *BRAF*V600E mutation to promote hematopoietic transformation. To this end, we performed targeted mutational analysis of a well-validated panel of 300 known cancer genes (18) (table S2) in genomic DNA from HCL leukemic cells and paired granulocyte samples from three HCL patients. We focused on mutations present in the HCL clone and not in paired granulocytes. This analysis revealed only the *BRAF*V600E mutation in one patient, *BRAF*V600E plus an *ARID1A* p.V1427fs mutation in another patient, and a *BRAF*V600E plus a *MLL3* p.C394Y mutation in a third patient. We then performed sequencing analysis by MiSeq for the *BRAF*V600E mutation and these additional alterations in HSCs (LN $CD34^+$ $CD38^-$ $CD90^+$ $CD45RA^-$), MPs (LN $CD19^-$ $CD10^-$ $CD34^+$ $CD38^+$), and hematogones (LN $CD34^+$ $CD38^{++}$) from the respective patients where these somatic mutations were identified in HCL cells. This analysis failed to reveal any mutation in the HSC or hematogone population other than the *BRAF*V600E mutation.

The identification of the *BRAF*V600E mutation in purified HSCs and progenitor B cells in HCL patients is highly suggestive of an immature cell of origin in HCL. To define the functional potential of *BRAF*V600E-mutant HSCs to give rise to HCL, we transplanted 3000 HSCs (LN $CD34^+$ $CD38^-$ $CD90^+$ $CD45RA^-$) from the BM aspirate of an untreated HCL patient into sublethally irradiated nonobese diabetic/severe combined immunodeficient interleukin-2 (IL-2) receptor γ chain knockout (NSG) mice (Fig. 2B). Serial flow cytometric and genetic analysis of human $CD45^+$ cells in the BM of engrafted mice at 6 months after transplantation revealed a population of $hCD45^+$ cells with an HCL immunophenotype ($hCD103^+$ $hCD11c^+$ $hCD19^+$) as well as immunophenotypic HSCs (LN $CD34^+$ $CD38^-$ $CD90^+$ $CD45RA^-$) (Fig. 2C). Moreover, genetic analysis of unfractionated $hCD45^+$ cells from the BM of engrafted mice revealed the presence of the *BRAF*V600E-mutant allele at a VAF of 4 and 9% in genomic DNA at 3 and 6 months after transplant, respectively (Fig. 2D). These data indicate that HSCs from HCL patients bearing the *BRAF*V600E mutation have functional self-renewal capacity, and strongly suggest that these cells give rise to HCL. Moreover, the self-renewal potential of *BRAF*-mutant HSCs and the fact that the

*BRAF*V600E mutation was detected in HSCs, hematogones, and HCL cells indicate that *BRAF*-mutant HSCs in HCL patients do not merely represent a subset of HCL cells.

Phenotypic analysis of mice with pan-hematopoietic versus B cell-restricted expression of *BRaf*V600E

We next sought to assess the effects of expressing *BRaf*V600E in different hematopoietic compartments in vivo. We used a conditional *BRaf*V600E murine model in which the mutant allele is expressed from the endogenous *BRaf* locus after Cre-mediated deletion of a lox-stop-lox cassette (19). *BRaf*V600E mice were crossed with *Mx1-cre*, *Vav-cre*, and *Cd19-cre* transgenic mice to delineate the effects of mutant *BRaf* expression in postnatal HSPCs, prenatal hematopoietic cells, and B lineage cells, respectively. *Mx1-cre BRaf*V600E mice developed a lethal hematopoietic disorder characterized by splenomegaly due to EMH [as previously reported (19)] and hepatomegaly (also due to EMH), anemia due to impaired erythroid differentiation, and thrombocytopenia by 3 weeks of age (Fig. 3, A to D, and fig. S2, A and B). The hematopoietic phenotype of *Mx1-cre BRaf*V600E was recapitulated when whole BM was transplanted into lethally irradiated recipient mice, consistent with a cell-autonomous phenotype (Fig. 3, A and B, and fig. S2A) (blood counts, spleen, and liver weights were analyzed 6 weeks after transplantation in 4-week-old lethally irradiated recipient mice to allow time for engraftment; spleen and liver weights were analyzed at 3 weeks of age in *Cd19-cre BRaf*V600E mice). In addition, mice with pan-hematopoietic *BRaf*V600E expression were marked by increased circulating soluble CD25 (sCD25) (Fig. 3E), a well-characterized tumor marker of HCL (6). sCD25 levels were significantly down-regulated ($P = 0.002$, Mann-Whitney U test) after therapy with the RAF inhibitor PLX4720. Because of a previously described high frequency of spontaneous Cre induction in the *Mx1-cre BRaf*V600E mice (19), we used tamoxifen-inducible mutant *BRaf* expression in the Cre-ER^T *BRaf*V600E model (which has minimal spontaneous excision) to characterize the latency of cell-autonomous hematopoietic abnormalities arising after Cre induction. BM cells from Cre-ER^T *BRaf*V600E or *BRaf*V600E *Cre*-negative control mice were transplanted into lethally irradiated recipients. Blood samples were taken from recipient mice 4 weeks after transplantation (at which time there were no significant differences between *Cre-ER^T BRaf*V600E and *BRaf*V600E cre-negative control mice), and then mice were treated with tamoxifen to activate expression of *BRaf*V600E. Two weeks after tamoxifen administration, *Cre-ER^T BRaf*V600E mice developed significant anemia ($P = 0.002$) and thrombocytopenia ($P = 0.02$) relative to control mice (fig. S2C).

Expression of *BRaf*V600E in fetal hematopoietic cells using the *Vav-cre* transgene resulted in 100% embryonic lethality (fig. S3A). Analysis of embryos generated from crossing *Vav-cre* transgenic mice to *BRaf*V600E mice revealed complete lethality of *Vav-cre BRaf*V600E embryos beyond day 12.5. At embryonic day 12.5, *Vav-cre BRaf*V600E embryos were observed at Mendelian ratios but were characterized by gross pallor, fetal liver necrosis, and a marked impairment of erythroid differentiation consistent with in utero hematopoietic transformation (fig. S3, B to E).

In contrast to the effects of *BRaf*V600E expression in HSPCs, conditional *BRaf*V600E expression in B lineage cells with *Cd19-cre* did not result in reduced survival or in an overt

hematopoietic phenotype. Mice sacrificed at 1 year of age had no overt phenotype outside of the B lineage, despite clear activation of mitogen-activated protein kinase (MAPK) signaling in B lineage cells (Fig. 3, A to D, and fig. S3, F and G). *Cd19-cre BRaf*V600E mice also had minimal elevation of sCD25 (Fig. 3E). These data demonstrate that restricting *BRaf*V600E expression to committed B lymphoid cells does not result in malignant transformation, suggesting that the phenotype of HCL is driven by alterations in HSPCs.

Effect of BRafV600E on HSC function and germinal center response to alloantigen

Given the expansion of HSCs noted in HCL patients, we next assessed the effects of expression of *BRaf*V600E on murine HSPC subsets (fig. S4). FACS analysis of HSPCs from the BM and spleen of secondarily transplanted *Mx1-cre BRaf*V600E mice and Cre-negative control mice revealed an increase in lineage-negative sca-1^+ c-kit^+ (LSK), LMPP, and common lymphoid progenitor (CLP) populations in the BM of knock-in mice relative to controls and a large increase in all HSPC populations in the spleen of knock-in mice relative to controls (consistent with EMH in *BRaf*V600E knock-in mice) (fig. S4).

We next sought to understand the effects of *BRaf*V600E expression on HSPC function and lineage specification. We plated unfractionated BM cells from *Mx1-cre BRaf*V600E mice in methylcellulose-containing myeloid and erythroid cytokines [IL-3, IL-6, stem cell factor (SCF), and erythropoietin (EPO)] or the lymphopoietic cytokine IL-7. *BRaf*V600E cells demonstrated impaired colony formation in myeloid and erythroid conditions. However, *BRaf*V600E BM exhibited serial replating capacity (>10 platings) in the presence of IL-7 (Fig. 4A). This increased clonogenic capacity was likewise observed using *Cd19-cre BRaf*V600E BM cells, suggesting increased self-renewal of an early B lineage population (fig. S5A). Accordingly, immunophenotyping of colonies capable of serially replating in IL-7-containing methylcellulose revealed predominantly pre-B cells and their progeny (fig. S5B). Given that LMPPs are poised in hematopoiesis between self-renewing HSCs and lymphoid and granulocyte/macrophage progenitors, we sought to examine the functional effects of *BRaf*V600E expression in this population. Purified LMPP cells (LSK $Flk2^+$) from *Mx1-cre BRaf*V600E mice acquired the ability to serially replate in IL-7-containing methylcellulose but exhibited impaired colony formation relative to control LMPP cells when plated in the presence of myeloid and erythroid cytokines (Fig. 4B). Together, these data suggest that *BRaf*V600E induces aberrant self-renewal in lymphoid precursor cells while impairing myeloid differentiation.

We next sought to determine the effect of alloantigen perturbation on the B cell phenotype of *BRaf*V600E-mutant mice. Four-week-old mice with B lineage expression of *BRaf*V600E were injected with T cell–dependent antigen sheep red blood cells (SRBCs) to induce germinal center (GC) formation. Analysis performed 10 days later (at which time the GC reaction is at its peak) revealed a significant ($P = 0.006$) increase in spleen weight, as well as the number and size of GC B cells in *BRaf*V600E mice relative to controls (Fig. 4, C and D). The GC response was more significant ($P = 0.02$) in Cd19-cre *BRaf*V600E mice compared to mice with GC-restricted expression of *BRaf*V600E (Cγ-cre *BRaf*V600E), suggesting that this enhanced response to antigenic stimulus arises from the effects of *BRaf*V600E in early B lineage cells rather than in mature B cells (Fig. 4, E and F).

Given the human and murine data demonstrating that *BRaf*V600E is acquired in HSCs in HCL, we investigated the effects of mutant *BRaf* on HSC self-renewal. We assessed the self-renewal of HSCs from CD45.2 *Mx1-cre BRaf*V600E or cre-negative *BRaf* V600E control mice in competitive repopulation assays. Four weeks after transplantation of equal numbers of *Mx1-cre BRaf*V600E BM cells and cre-negative control cells into lethally irradiated recipient mice, the CD45.2 peripheral blood (PB) chimerism of mice transplanted with CD45.2 *Mx1-cre BRaf*V600E BM was greatly reduced compared to control (Fig. 4, G and H). At the same time point, the proportion of CD45.2 cells that were $B220^+$ B lineage cells was higher in mice transplanted with *Mx1-cre BRaf*V600E CD45.2-positive cells compared to controls (Fig. 4G). Sixteen weeks after transplantation, the proportion of *Mx1-cre BRaf*V600E CD45.2 cells was similar to cre-negative controls, consistent with intact self-renewal of *BRaf*V600E HSCs (Fig. 4H). Mice transplanted with *Mx1-cre BRaf*V600E CD45.2-positive cells developed anemia and thrombocytopenia by 16 weeks after transplantation, a phenotype similar to that which was observed in primary *Mx1-cre BRaf*V600E mice and noncompetitive transplants (Fig. 4I). To exclude an effect of homing or engraftment on the function of *BRaf*V600E BM cells in vivo, we performed competitive transplantation of *Cre-ER^T BRaf*V600E BM cells followed by cre-mediated expression of the mutant allele 4 weeks after transplantation, demonstrating a significant ($P = 0.006$ at 16 weeks after transplantation) competitive advantage of *Cre-ER^T BRaf*V600E BM cells (fig. S5C).

Effect of BRAF inhibition on *BRAF*-mutant HSPCs and hematopoietic differentiation

The above genetic and functional data suggest that *BRaf*V600E mutations alter the differentiation and self-renewal potential of HSPCs and that the ensuing lymphoid transformation and block in myeloid and erythroid differentiation result in phenotypic HCL (although cells with classic hairy cell–like morphology were not seen in the murine models). Recent case reports have noted that HCL patients respond to inhibition of mutant BRAF with vemurafenib, as assessed by a reduction in morphologic hairy cells and a reduction in splenomegaly (20, 21). We therefore investigated the effect of vemurafenib on *BRAF*V600E-mutant HSPCs using murine models and relapsed/refractory HCL patients treated on a phase 2 study of vemurafenib. PLX4720 treatment of wild-type mice transplanted with *Mx1-Cre$^+$ BRaf*V600E-mutant BM cells improved anemia, reduced hepatosplenomegaly, and attenuated B cell clonogenic capacity (Fig. 5, A to D, and fig. S6, A to F). In the clinical context, vemurafenib treatment normalized HSPC frequencies within 3 months of starting therapy (Fig. 5, E and F). Patients treated with vemurafenib had restoration of normal myelopoiesis with BRAF inhibition, demonstrating that the impaired myeloid differentiation in HCL is dependent on mutant *BRAF*V600E signaling (Fig. 5, G and H). Vemurafenib treatment restored the myeloid colony-forming ability of sorted HSCs (LN $CD34^+$ $CD38^-$ $CD90^+$ $CD45RA^-$) and MPs (LN $CD34^+$ $CD38^+$) isolated from HCL patients compared to pretreatment marrows (fig. S6G), suggesting that the improvement in myeloid and erythroid progenitor output in vivo is cell-autonomous.

DISCUSSION

The hallmark leukemic cell in HCL has frequently been considered to be derived from a postgerminal B cell, given that these cells express switched immunoglobulin isotypes (1), with immunoglobulin variable genes that have undergone somatic hypermutation in most patients (3, 22). At the same time, many features of HCL are not consistent with origin from a postgerminal B cell, such as their unique immunophenotype and morphology, as well as decreased hematopoietic output that is often out of proportion to HCL disease burden in the BM. By tracing the origin of a specific somatic aberration characteristic of HCL, we have identified a clear link in the pathogenesis of HCL to an oncogenic disease allele acquired in the HSC compartment. Functional studies with human and murine *BRAF*V600E-mutant HSCs further demonstrated that the *BRAF* mutation affects the differentiation and function of different committed hematopoietic progenitors, which may drive the disease phenotype.

Although HCL is a relatively rare malignancy, the present data further demonstrate that mature B cell malignancies can initiate in the HSC compartment. Although the stem cell origin for myeloid malignancies such as myeloproliferative neoplasms, myelodysplastic syndromes, and acute myeloid leukemia (AML) is well established, a link between aberrations in HSPCs and development of mature lymphoid malignancies has been less thoroughly investigated. One reason for this is that, unlike mature myeloid cells, subsets of normal mature B cells are characterized by the capacity to self-renew and differentiate as part of their normal function. For example, the function of memory B cells is to self-renew and generate differentiated progeny in response to antigenic stimuli. Thus, the paradigm of linking B cell malignancies to counterparts in normal B cell development has been a predominant model to describe the cell of origin for these disorders and may have obscured the identification of a more primitive cell of origin. Emerging evidence suggests that HSPCs may play important roles in other neoplasms of mature B cells. For example, multiple myeloma, a disorder considered to be a malignancy of late-stage immunoglobulin-secreting plasma cells, was recently found to contain subpopulations of pre-plasmablasts and $CD20^+$ B cell progenitors, which propagate the disorder and mediate treatment resistance (23). Similarly, Kikushige *et al.* recently demonstrated that the propensity to generate clonal B cells in patients with the mature B cell malignancy CLL is acquired in the HSC compartment (24). Recent genomic analyses of leukemias of another lymphoid lineage, T cell acute lymphoblastic leukemia (T-ALL), revealed that a specific subset of T-ALL is highly similar to normal and myeloid leukemic HSCs in gene expression and mutational profile (25). Collectively, these findings suggest that genomic and functional analyses of lymphoid malignancies may reveal unexpected alterations in less differentiated HSPC populations.

In the studies by Kikushige *et al.*, xenotransplantation of HSCs from CLL patients gave rise to engraftment of mono- and oligoclonal cell populations with a CLL-like phenotype, but the resulting clones were genetically disparate from the original CLL clones seen in the leukemic cells originally isolated from patients. One potential explanation for this finding is that additional genetic abnormalities acquired along the course of hematopoiesis might be essential in giving rise to the clonal CLL disorder (24, 26). Similarly, here, although *BRaf*V600E expression in HSPCs resulted in increased clonogenic capacity of early B cell

populations, as well as anemia, thrombocytopenia, and EMH, no cells with a morphologic phenotype of hairy cells were seen in any murine model studied. This suggests that the development of additional co-occurring genetic alterations along the course of hematopoiesis may be necessary to give rise to mature HCL cells. Alternatively, the level of expression and/or functional role of BRAF in hematopoiesis may be incompletely conserved between mouse and human.

There are several limitations of this study to note. First, we attempted to address the question of whether there is a hierarchy of additional genetic alterations co-occurring with the *BRAF*V600E mutation in HCL patients. Targeted sequencing analysis of 300 cancer-associated genes in three HCL samples revealed only two additional somatic mutations co-occurring with the *BRAF*V600E mutation in HCL cells, neither of which were present in HSCs from the same individual. These data are consistent with the *BRAFV600E* mutation representing an early or inciting event in HCL pathogenesis. This is analogous to recently described preleukemic HSCs from AML patients who harbor somatic mutations in frequently mutated genes such as *DNMT3A* (27, 28). In such a scenario, a preleukemic HSC clone in HCL might acquire subsequent additional genetic alterations in HSCs, B cell progenitors, or mature B cells, resulting in the appearance of a mature B cell clone that undergoes characteristic immunoglobulin rearrangement and eventually proliferates to manifest as clinically apparent HCL. However, a more extensive mutational analysis of HCL cells and paired HSPCs will be needed to more definitively address this question. Moreover, our use of granulocyte DNA as matched somatic tissue may have obscured additional mutations acquired early in the hematopoietic compartment and present at similar frequencies in granulocyte and HCL DNA. Second, although our analyses of the VAF of the *BRAF*V600E mutation demonstrated the presence of the *BRAF* mutation in HSPC subsets from HCL patients, these analyses used cDNA, where the level of wild-type and mutant *BRAF* expression may differ from the VAF at the level of genomic DNA in these cell subsets.

Data from the murine models studied here and flow cytometric characterization of the BM of HCL patients suggest that the cytopenias seen in HCL patients are due in part to HSPC-intrinsic effects of the *BRAF*V600E mutation on erythropoiesis, megakaryopoiesis, and myelopoiesis. Moreover, these data suggest that the use of therapies targeting MAPK signaling in HCL may lead to durable remissions not only through effects on mature leukemic cells but also through targeted inhibition of signaling and survival in mutant HSPCs. Indeed, treatment of both murine models and HCL patients with RAF inhibition resulted in improvements in myelopoiesis and erythropoiesis, as well as restoration of aberrant HSPC frequencies. Our results predict that therapeutic mutant BRAF inhibition will have the capability to induce durable remissions and restoration of normal hematopoiesis in HCL.

MATERIALS AND METHODS

Study design and patients

The goal of this study was to understand the cell of origin of HCL through the use of (i) genetic analysis of specific hematopoietic subsets from the BM and blood of HCL patients,

(ii) comparison of the effects on hematopoiesis of activating the *BRaf*V600E mutation in various hematopoietic cell subsets in mice, and (iii) analysis of the effects of targeting vemurafenib on hematopoiesis in patients with HCL treated longitudinally with vemurafenib and in *BRaf*V600E mice treated in vivo with vemurafenib.

Patient samples were obtained from patients with newly diagnosed or relapsed HCL seen at Memorial Sloan Kettering Cancer Center. The effect of vemurafenib on stem cell number, function, and hematopoietic reconstitution in vivo was studied using patient samples from an ongoing phase 2 clinical trial of vemurafenib in relapsed or refractory HCL ("A phase II study of the BRAF inhibitor, vemurafenib, in patients with relapsed or refractory hairy cell leukemia," ClinicalTrials.gov identifier NCT01711632). The study is ongoing and being conducted according to the Declaration of Helsinki and with approval from the Institutional Review Board of Memorial Sloan Kettering Cancer Center. All patients had HCL refractory to standard therapy and met all inclusion and exclusion criteria. All provided written informed consent before participating in this study. This study involves exposure to vemurafenib at a dose of 960 mg orally twice a day in back-to-back cycles of 4 weeks (28 days) for at least three cycles. A BM aspirate and/or biopsy is performed before treatment and after the first cycle. After the completion of the third cycle, a repeat BM aspirate and/or biopsy is performed for assessment of response and evaluation of minimal residual disease. If either morphologic or minimal residual disease is evident, an additional three cycles of vemurafenib are given for a maximum of six cycles total.

Experiments analyzing human hematopoietic cell subsets pretreated with vemurafenib (Fig. 1) involved 14 individual HCL patients and 3 normal age-matched controls (table S1). Analysis of the effects of vemurafenib therapy on hematopoiesis longitudinally in clinical trial specimens involved four to six patient samples per group (Fig. 5, F and G) or one to three representative patient samples (Fig. 5, E and H).

All murine experiments were done using 3 to 10 animals per group in each experiment, and all experiments were performed at least three times except where noted. For murine drug experiments, animals were randomly allocated to drug treatment or vehicle treatment, and treatment was administered in an unblinded fashion.

Antibodies and FACS analysis of human and murine cells

Details of all antibodies (for both human and mouse studies) used for FACS and Western blot analyses are located in the Supplementary Materials.

Animals, in vivo studies, and in vivo drug treatment of mice

All animals were housed at Memorial Sloan Kettering Cancer Center. All animal procedures were conducted in accordance with the Guidelines for the Care and Use of Laboratory Animals and were approved by the Institutional Animal Care and Use Committees at Memorial Sloan Kettering Cancer Center.

Mice with conditional expression of *BRaf*V600E (LSL-*BRaf*V600E) from its endogenous locus were originally created and described by Mercer *et al.* (19). LSL-BRafV600E mice on a pure C57BL/6 background were crossed to interferon-α–inducible *Mx1-cre* mice (The

Jackson Laboratory), hematopoietic-specific *Vav-cre* mice, B lineage *Cd19-cre* mice, GC-restricted *Cγ-cre* mice, and tamoxifen-inducible pCMV*Cre-ER*^{T} mice (described as *Cre-ER*^{T} in the article) (29-33). All Cre strains listed above were on a pure C57BL/6 background. Further details of transplantation analyses and in vivo drug studies in mice are listed in the Supplementary Materials.

NSG xenotransplantation assay

FACS-purified cells were transplanted by retro-orbital injection into 6-week-old NSG mice (The Jackson Laboratory) conditioned with 225 rads of irradiation. BM aspirates were performed at 3 and 6 months after transplantation, and cells were then analyzed for human engraftment (hCD45$^+$) that was further characterized for human HSC markers (hCD34, hCD38, hCD90, hCD45RA) and HCL markers (hCD19, hCD103, hCD11c).

*BRAF*V600E allele-specific PCR analysis and quantitative sequencing

Allele-specific oligonucleotide PCR analysis for detection of the *BRAF*V600E mutation was performed as described previously (14), using cDNA generated from RNA of sorted cell populations. After amplification of PCR products, Sanger sequencing of PCR products generated from amplification using wild-type forward (5′-TAGGTGATTTTGGTCTAGCTACCGT-3′) and common reverse primer (5′-GTAACTCAGCAGCATCTCAGGG-3′), as well as using mutant-specific forward (5′-TAGGTGATTTTGGTCTAGCTACCGA-3′) and common reverse primer, was performed. The presence of amplified PCR products using the mutant-selective forward primer and common reverse primer with clear evidence of the *BRAF*V600E mutation in Sanger sequencing electropherograms indicated detection of the *BRAF*V600E mutation.

Quantitative sequencing analysis was performed by first preparing libraries with cDNA or genomic DNA from sorted hematopoietic cell subsets from HCL patients using the Kapa Biosystems Library Preparation Kit. In some instances, cDNA was amplified before library preparation using Kapa HiFi PCR kit followed by Agencourt AMPure bead purification (Beckman Coulter). Libraries were pooled equimolarly and sequenced on an Illumina MiSeq. Sequencing was performed at a median depth of >1000× to identify mutations with VAF of >1% (variants present at VAF<1% were not considered informative).

Sequencing analysis of mutations co-occurring with *BRAF*V600E mutation in HCL We used standard techniques to extract genomic DNA from flow-sorted HCL and granulocyte cells. Barcoded, massively parallel sequencing libraries were prepared (New England Biolabs, Kapa Biosystems), and exon capture was performed on barcoded pools (NimbleGen Seq-Cap) according to the manufacturer's directions. Briefly, we designed and synthesized synthetic DNA probes complementary to the coding sequence of 300 genes known to undergo somatic genomic alterations in cancer (table S2). Genomic DNA libraries were subjected to solution-phase hybrid capture using the DNA probes, followed by massively parallel sequencing on the Illumina HiSeq 2500. We sequenced 100 bases from both ends of library DNA fragments, achieving about 15 million purity filtered reads per sample. Paired reads were aligned to the reference human genome (hg19) using the Burrows-Wheeler Alignment tool (34) and postprocessed using the Genome Analysis Toolkit according to best

practices (35). Single-nucleotide variants were called using MuTect (36), and indels were called using SomaticIndelDetector (35). All alterations were manually reviewed using the Integrative Genomics Viewer (37).

In vitro colony-forming assays

Details of all methylcellulose colony assays using human or mouse hematopoietic cells are described in the Supplementary Materials.

Histological analyses

Mice were sacrificed and dissected to harvest sternum, femurs, tibiae, spleen, and liver. Tissue samples were fixed for 24 hours in 4% paraformaldehyde, dehydrated, and embedded in paraffin. Paraffin blocks were sectioned at 4 μm and stained with hematoxylin and eosin. Cytospins were performed by resuspending cell pellets in warm phosphate-buffered saline. Cells were then spun onto 3 × 1-inch frosted microscope slides (Fisher Scientific) at 350*g* for 5 min. Slides were air-dried and stained using the Giemsa-Wright method (38). Images were acquired using a Zeiss Axio Observer A1 microscope.

sCD25 receptor measurement

sCD25 concentration was measured in serum from PB using a previously validated Luminex assay (39). Luminex assays were then carried out using the FLEXMAP 3D multiplexing platform (Luminex xMAP system). Serum samples were prepared according to the manufacturer's instructions.

Statistical analysis

Values reported represent means ± SD (or ±SEM, where noted). *P* values were calculated with GraphPad Prism, with $P < 0.05$ considered significant. Fisher's exact test (two-tailed) or the Mann-Whitney *U* test (two-tailed, unpaired) was used to compare blood cell counts, organ weights, and cell frequencies determined by FACS. Experiments were done three to five times except where noted, and the particular statistical analyses used in the experiments are noted in the figure captions. Statistics were performed to illustrate significance between groups where $n \geq 3$.

Supplementary Material

Refer to Web version on PubMed Central for supplementary material.

Acknowledgments

We thank C. Pritchard for permission to use the *BRaf*V600E conditional lox-stop-lox model.

Funding: This work was supported by a grant from the Geoffrey Beene Cancer Foundation to J.H.P. and O.A.-W. O.A.-W. is supported by an NIH K08 Clinical Investigator Award (1K08CA160647-01), a U.S. Department of Defense Postdoctoral Fellow Award in Bone Marrow Failure Research (W81XWH-12-1-0041), the Josie Roberston Clinical Investigator Program, and a Damon Runyon Clinical Investigator Award with Support from the Evans Foundation. S.S.C. is supported by a Young Investigator Award from the American Society of Clinical Oncology and a U.S. Department of Defense Postdoctoral Fellow Award in Bone Marrow Failure Research (BM120096). J.H.P. is supported by a Special Fellow Award in Clinical Research from the Leukemia and Lymphoma Society.

REFERENCES AND NOTES

1. Golomb H, Davis S, Wilson C, Vardiman J. Surface immunoglobulins on hairy cells of 55 patients with hairy cell leukemia. Am. J. Hematol. 1982; 12:397–401. [PubMed: 7114052]
2. Forconi F, Sahota S, Raspadori D, Mockridge C, Lauria F, Stevenson F. Tumor cells of hairy cell leukemia express multiple clonally related immunoglobulin isotypes via RNA splicing. Blood. 2001; 98:1174–1181. [PubMed: 11493467]
3. Maloum K, Magnac C, Azgui Z, Cau C, Charlotte F, Binet J, Merle-Béral H, Dighiero G. VH gene expression in hairy cell leukaemia. Br. J. Haematol. 1998; 101:171–178. [PubMed: 9576198]
4. Polliack A. Hairy cell leukemia: Biology, clinical diagnosis, unusual manifestations and associated disorders. Rev. Clin. Exp. Hematol. 2002; 6:366–388. [PubMed: 12823778]
5. Tiacci E, Liso A, Piris M, Falini B. Evolving concepts in the pathogenesis of hairy-cell leukaemia. Nat. Rev. Cancer. 2006; 6:437–448. [PubMed: 16723990]
6. Janik J. Tumor markers in hairy cell leukemia. Leuk. Lymphoma. 2011; 52(Suppl. 2):69–71. [PubMed: 21463109]
7. Juliusson G, Lenkei R, Liliemark J. Flow cytometry of blood and bone marrow cells from patients with hairy cell leukemia: Phenotype of hairy cells and lymphocyte subsets after treatment with 2-chlorodeoxyadenosine. Blood. 1994; 83:3672–3681. [PubMed: 7911341]
8. Basso K, Liso A, Tiacci E, Benedetti R, Pulsoni A, Foa R, Di Raimondo F, Ambrosetti A, Califano A, Klein U, Dalla Favera R, Falini B. Gene expression profiling of hairy cell leukemia reveals a phenotype related to memory B cells with altered expression of chemokine and adhesion receptors. J. Exp. Med. 2004; 199:59–68. [PubMed: 14707115]
9. Anderson K, Boyd A, Fisher D, Leslie D, Schlossman S, Nadler L. Hairy cell leukemia: A tumor of pre-plasma cells. Blood. 1985; 65:620–629. [PubMed: 3871642]
10. Burke J, Sheibani K. Hairy cells and monocytoid B lymphocytes: Are they related? Leukemia. 1987; 1:298–300. [PubMed: 3118107]
11. Thorsélius M, Walsh S, Thunberg U, Hagberg H, Sundström C, Rosenquist R. Heterogeneous somatic hypermutation status confounds the cell of origin in hairy cell leukemia. Leuk. Res. 2005; 29:153–158. [PubMed: 15607363]
12. van den Oord J, de Wolf-Peeters C, Desmet V. Hairy cell leukemia: A B-lymphocytic disorder derived from splenic marginal zone lymphocytes? Blut. 1985; 50:191–194. [PubMed: 3872689]
13. Tiacci E, Trifonov V, Schiavoni G, Holmes A, Kern W, Martelli M, Pucciarini A, Bigerna B, Pacini R, Wells V, Sportoletti P, Pettirossi V, Mannucci R, Elliott O, Liso A, Ambrosetti A, Pulsoni A, Forconi F, Trentin L, Semenzato G, Inghirami G, Capponi M, Di Raimondo F, Patti C, Arcaini L, Musto P, Pileri S, Haferlach C, Schnittger S, Pizzolo G, Foà R, Farinelli L, Haferlach T, Pasqualucci L, Rabadan R, Falini B. *BRAF* mutations in hairy-cell leukemia. N. Engl. J. Med. 2011; 364:2305–2315. [PubMed: 21663470]
14. Arcaini L, Zibellini S, Boveri E, Riboni R, Rattotti S, Varettoni M, Guerrera M, Lucioni M, Tenore A, Merli M, Rizzi S, Morello L, Cavalloni C, Da Vià M, Paulli M, Cazzola M. The *BRAF*V600E mutation in hairy cell leukemia and other mature B-cell neoplasms. Blood. 2012; 119:188–191. [PubMed: 22072557]
15. Schnittger S, Bacher U, Haferlach T, Wendland N, Ulke M, Dicker F, Grossmann V, Haferlach C, Kern W. Development and validation of a real-time quantification assay to detect and monitor BRAFV600E mutations in hairy cell leukemia. Blood. 2012; 119:3151–3154. [PubMed: 22331186]
16. Goardon N, Marchi E, Atzberger A, Quek L, Schuh A, Soneji S, Woll P, Mead A, Alford KA, Rout R, Chaudhury S, Gilkes A, Knapper S, Beldjord K, Begum S, Rose S, Geddes N, Griffiths M, Standen G, Sternberg A, Cavenagh J, Hunter H, Bowen D, Killick S, Robinson L, Price A, Macintyre E, Virgo P, Burnett A, Craddock C, Enver T, Jacobsen SE, Porcher C, Vyas P. Coexistence of LMPP-like and GMP-like leukemia stem cells in acute myeloid leukemia. Cancer Cell. 2011; 19:138–152. [PubMed: 21251617]
17. Doulatov S, Notta F, Eppert K, Nguyen LT, Ohashi PS, Dick JE. Revised map of the human progenitor hierarchy shows the origin of macrophages and dendritic cells in early lymphoid development. Nat. Immunol. 2010; 11:585–593. [PubMed: 20543838]

18. Won HH, Scott SN, Brannon AR, Shah RH, Berger MF. Detecting somatic genetic alterations in tumor specimens by exon capture and massively parallel sequencing. J. Vis. Exp. 2013:e50710. [PubMed: 24192750]
19. Mercer K, Giblett S, Green S, Lloyd D, DaRocha Dias S, Plumb M, Marais R, Pritchard C. Expression of endogenous oncogenic ^{V600E}*B-raf* induces proliferation and developmental defects in mice and transformation of primary fibroblasts. Cancer Res. 2005; 65:11493–11500. [PubMed: 16357158]
20. Dietrich S, Glimm H, Andrulis M, von Kalle C, Ho A, Zenz T. BRAF inhibition in refractory hairy-cell leukemia. N. Engl. J. Med. 2012; 366:2038–2040. [PubMed: 22621641]
21. Munoz J, Schlette E, Kurzrock R. Rapid response to vemurafenib in a heavily pretreated patient with hairy cell leukemia and a *BRAF* mutation. J. Clin. Oncol. 2013; 31:e351–e352. [PubMed: 23733763]
22. Vanhentenrijk V, Tierens A, Wlodarska I, Verhoef G, Wolf-Peeters C. V_H gene analysis of hairy cell leukemia reveals a homogeneous mutation status and suggests its marginal zone B-cell origin. Leukemia. 2004; 18:1729–1732. [PubMed: 15356640]
23. Leung-Hagesteijn C, Erdmann N, Cheung G, Keats JJ, Stewart AK, Reece DE, Chung KC, Tiedemann RE. Xbp1s-negative tumor B cells and pre-plasmablasts mediate therapeutic proteasome inhibitor resistance in multiple myeloma. Cancer Cell. 2013; 24:289–304. [PubMed: 24029229]
24. Kikushige Y, Ishikawa F, Miyamoto T, Shima T, Urata S, Yoshimoto G, Mori Y, Iino T, Yamauchi T, Eto T, Niiro H, Iwasaki H, Takenaka K, Akashi K. Self-renewing hematopoietic stem cell is the primary target in pathogenesis of human chronic lymphocytic leukemia. Cancer Cell. 2011; 20:246–259. [PubMed: 21840488]
25. Zhang J, Ding L, Holmfeldt L, Wu G, Heatley SL, Payne-Turner D, Easton J, Chen X, Wang J, Rusch M, Lu C, Chen SC, Wei L, Collins-Underwood JR, Ma J, Roberts KG, Pounds SB, Ulyanov A, Becksfort J, Gupta P, Huether R, Kriwacki RW, Parker M, McGoldrick DJ, Zhao D, Alford D, Espy S, Bobba KC, Song G, Pei D, Cheng C, Roberts S, Barbato MI, Campana D, Coustan-Smith E, Shurtleff SA, Raimondi SC, Kleppe M, Cools J, Shimano KA, Hermiston ML, Doulatov S, Eppert K, Laurenti E, Notta F, Dick JE, Basso G, Hunger SP, Loh ML, Devidas M, Wood B, Winter S, Dunsmore KP, Fulton RS, Fulton LL, Hong X, Harris CC, Dooling DJ, Ochoa K, Johnson KJ, Obenauer JC, Evans WE, Pui CH, Naeve CW, Ley TJ, Mardis ER, Wilson RK, Downing JR, Mullighan CG. The genetic basis of early T-cell precursor acute lymphoblastic leukaemia. Nature. 2012; 481:157–163. [PubMed: 22237106]
26. Alizadeh A, Majeti R. Surprise! HSC are aberrant in chronic lymphocytic leukemia. Cancer Cell. 2011; 20:135–136. [PubMed: 21840478]
27. Shlush LI, Zandi S, Mitchell A, Chen WC, Brandwein JM, Gupta V, Kennedy JA, Schimmer AD, Schuh AC, Yee KW, McLeod JL, Doedens M, Medeiros JJ, Marke R, Kim HJ, Lee K, McPherson JD, Hudson TJ, Brown AM, Trinh QM, Stein LD, Minden MD, Wang JC, Dick JE. Identification of pre-leukaemic haematopoietic stem cells in acute leukaemia. Nature. 2014; 506:328–333. [PubMed: 24522528]
28. Corces-Zimmerman MR, Hong WJ, Weissman IL, Medeiros BC, Majeti R. Preleukemic mutations in human acute myeloid leukemia affect epigenetic regulators and persist in remission. Proc. Natl. Acad. Sci. U.S.A. 2014; 111:2548–2553. [PubMed: 24550281]
29. Kühn R, Schwenk F, Aguet M, Rajewsky K. Inducible gene targeting in mice. Science. 1995; 269:1427–1429. [PubMed: 7660125]
30. Lakso M, Pichel JG, Gorman JR, Sauer B, Okamoto Y, Lee E, Alt FW, Westphal H. Efficient in vivo manipulation of mouse genomic sequences at the zygote stage. Proc. Natl. Acad. Sci. U.S.A. 1996; 93:5860–5865. [PubMed: 8650183]
31. Stadtfeld M, Graf T. Assessing the role of hematopoietic plasticity for endothelial and hepatocyte development by non-invasive lineage tracing. Development. 2005; 132:203–213. [PubMed: 15576407]
32. Casola S, Cattoretti G, Uyttersprot N, Koralov S, Seagal J, Segal J, Hao Z, Waisman A, Egert A, Ghitza D, Rajewsky K. Tracking germinal center B cells expressing germ-line immunoglobulin γ1 transcripts by conditional gene targeting. Proc. Natl. Acad. Sci. U.S.A. 2006; 103:7396–7401. [PubMed: 16651521]

33. Feil R, Brocard J, Mascrez B, LeMeur M, Metzger D, Chambon P. Ligand-activated site-specific recombination in mice. Proc. Natl. Acad. Sci. U.S.A. 1996; 93:10887–10890. [PubMed: 8855277]

34. Li H, Durbin R. Fast and accurate short read alignment with Burrows–Wheeler transform. Bioinformatics. 2009; 25:1754–1760. [PubMed: 19451168]

35. DePristo M, Banks E, Poplin R, Garimella K, Maguire J, Hartl C, Philippakis A, del Angel G, Rivas M, Hanna M, McKenna A, Fennell T, Kernytsky A, Sivachenko A, Cibulskis K, Gabriel S, Altshuler D, Daly M. A framework for variation discovery and genotyping using next-generation DNA sequencing data. Nat. Genet. 2011; 43:491–498. [PubMed: 21478889]

36. Cibulskis K, Lawrence M, Carter S, Sivachenko A, Jaffe D, Sougnez C, Gabriel S, Meyerson M, Lander E, Getz G. Sensitive detection of somatic point mutations in impure and heterogeneous cancer samples. Nat. Biotechnol. 2013; 31:213–219. [PubMed: 23396013]

37. Thorvaldsdóttir H, Robinson J, Mesirov J. Integrative Genomics Viewer (IGV): High-performance genomics data visualization and exploration. Brief. Bioinform. 2013; 14:178–192. [PubMed: 22517427]

38. Strober W. Wright-Giemsa and nonspecific esterase staining of cells. Curr. Protoc. Cytom. 2001 Appendix 3, Appendix 3D.

39. Russell SE, Moore AC, Fallon PG, Walsh PT. Soluble IL-2Rα (sCD25) exacerbates auto-immunity and enhances the development of Th17 responses in mice. PLOS One. 2012; 7:e47748. [PubMed: 23077668]

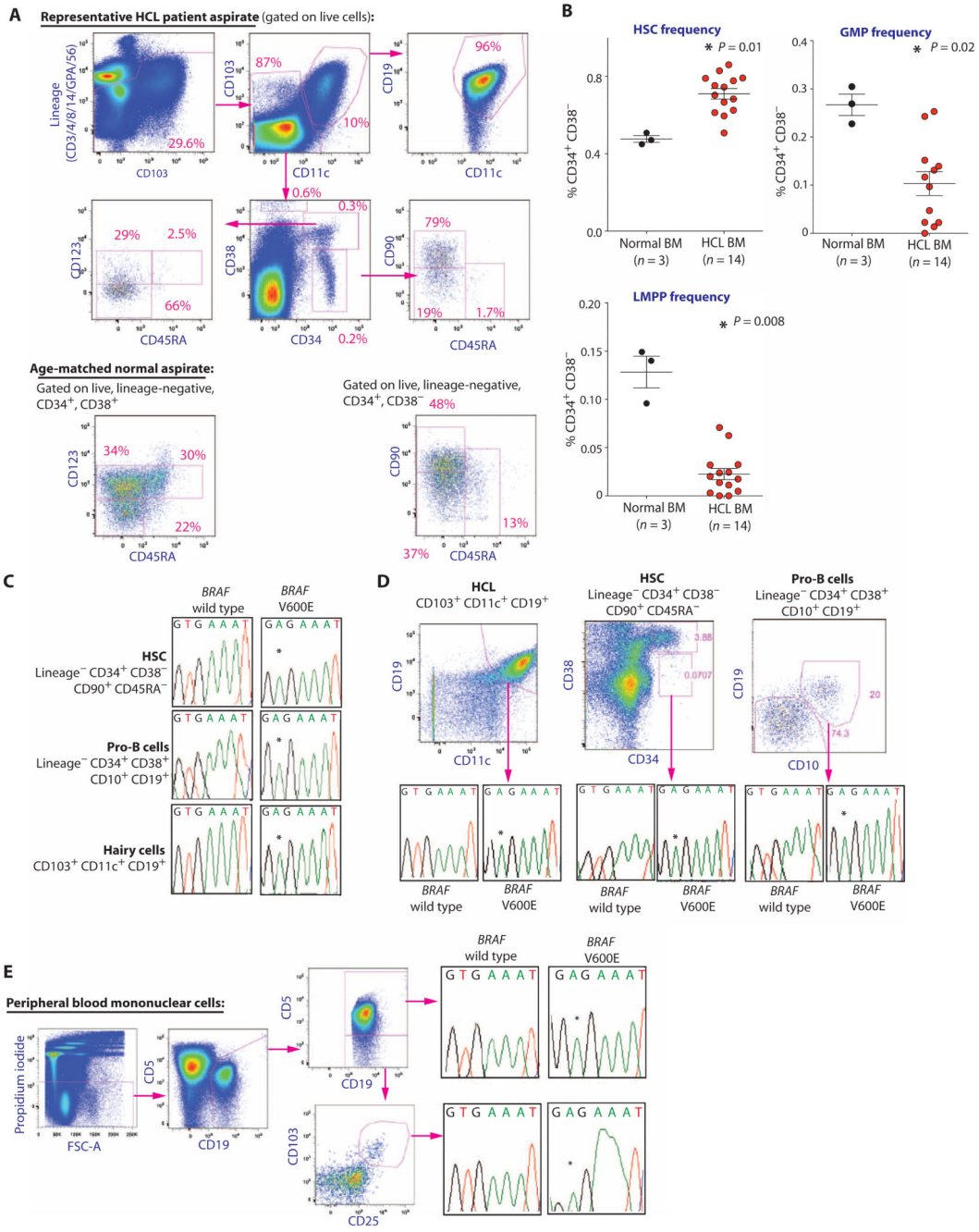

Fig. 1. HSPC abnormalities and the presence of the *BRAF*V600E mutation in HSCs of HCL patients

(**A**) Stem and progenitor flow cytometric analysis of the BM of a representative HCL patient and an age-matched control. The sort schema shown was used for isolation of HCL cells ($CD103^+$ $CD19^+$ $CD11c^+$ cells), HSCs (LN $CD34^+$ $CD38^-$ $CD90^+$ $CD45RA^-$ cells), hematogones ($CD34^-$ $CD38^{++}$ $CD10^+$ $CD19^+$), and MP cells (LN $CD34^+$ $CD38^+$ $CD45RA^{+/-}$ $CD123^{+/-}$ cells). (**B**) Frequencies of HSCs, LMPPs (LN $CD34^+$ $CD38^-$ $CD90^-$ $CD45RA^+$), and GMPs (LN $CD34^+$ $CD38^+$ $CD123^+$ $CD45RA^+$) in 14 patients with HCL

and 3 age-matched normal control BM aspirate samples. (**C**) Prospective cell separation including double sorting to ensure purity and lack of HCL cell contamination followed by allele-specific polymerase chain reaction (PCR) analysis for the presence of the *BRAF*V600E mutation reveals the mutation in HSCs, pro-B cells, and HCL cells. (**D**) Similar data from a second HCL patient revealing the mutation in HSC, pro-B, and HCL double-sorted cell populations. (**E**) Prospective isolation of CLL ($CD19^+$ $CD5^+$ $CD103^-$ $CD11c^-$ cells) and HCL cell populations ($CD19^+$ $CD103^+$ $CD11c^+$ $CD5^-$ cells) from the PB of one individual with both disorders reveals the *BRAF*V600E mutation in both cell populations. Error bars represent means ± SD. $*P < 0.05$ (Mann-Whitney *U* test).

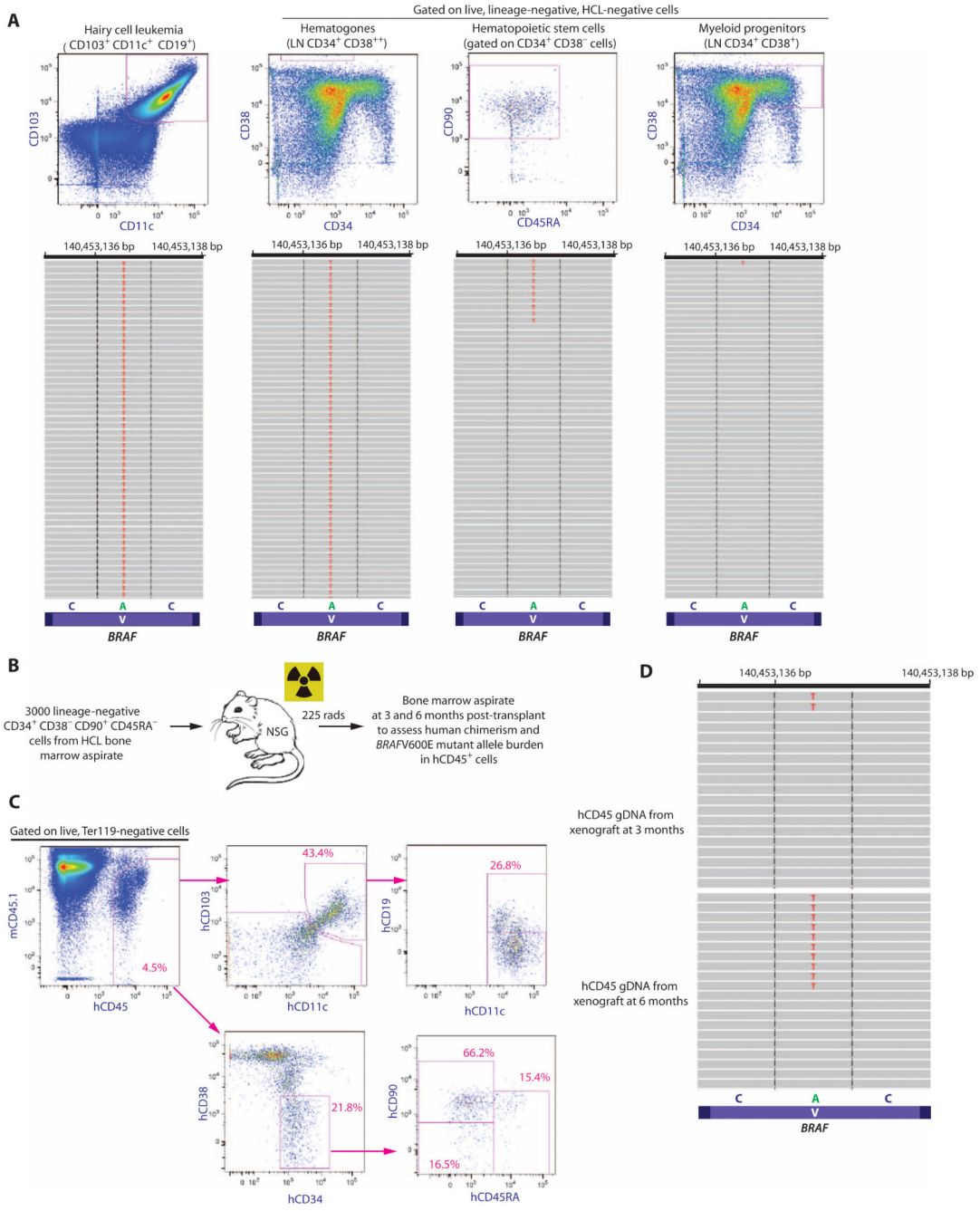

Fig. 2. Quantitative analysis of the *BRAF*V600E mutation in HSCs from HCL patients and functional self-renewal capacity of *BRAF*V600E-mutant HSCs

(**A**) Representative FACS analysis and quantitative sequencing analysis revealing the VAF of the *BRAF* c.T1860A p.V600E mutation in HCL cells, hematogones, HSCs, and MP cells from an HCL patient (for clarity, only 52 reads are displayed). cDNA from double FACS-sorted cell populations were used for MiSeq targeted sequencing. (**B**) Schema of xenograft experiment where 3000 HSCs from a *BRAF*V600E-mutant HCL patient were injected into sublethally irradiated NSG mice followed by flow cytometric analysis of human engraftment

and HCL cells, as well as quantification of the *BRAF*V600E mutation by sequencing analysis. (**C**) At 6 months after transplant, overall human chimerism was 4.5% with the presence of human HSCs ($hCD45^+$ $hCD34^+$ $hCD38^-$ $hCD90^+$ $hCD45RA^-$) and a cell population with the immunophenotype of HCL cells ($hCD45^+$ $hCD103^+$ $hCD19^+$ $hCD11c^+$). (**D**) MiSeq sequencing analysis at 100× coverage reveals *BRAF*V600E mutation in 4 and 9% of $hCD45^+$ cell genomic DNA at 3 and 6 months, respectively.

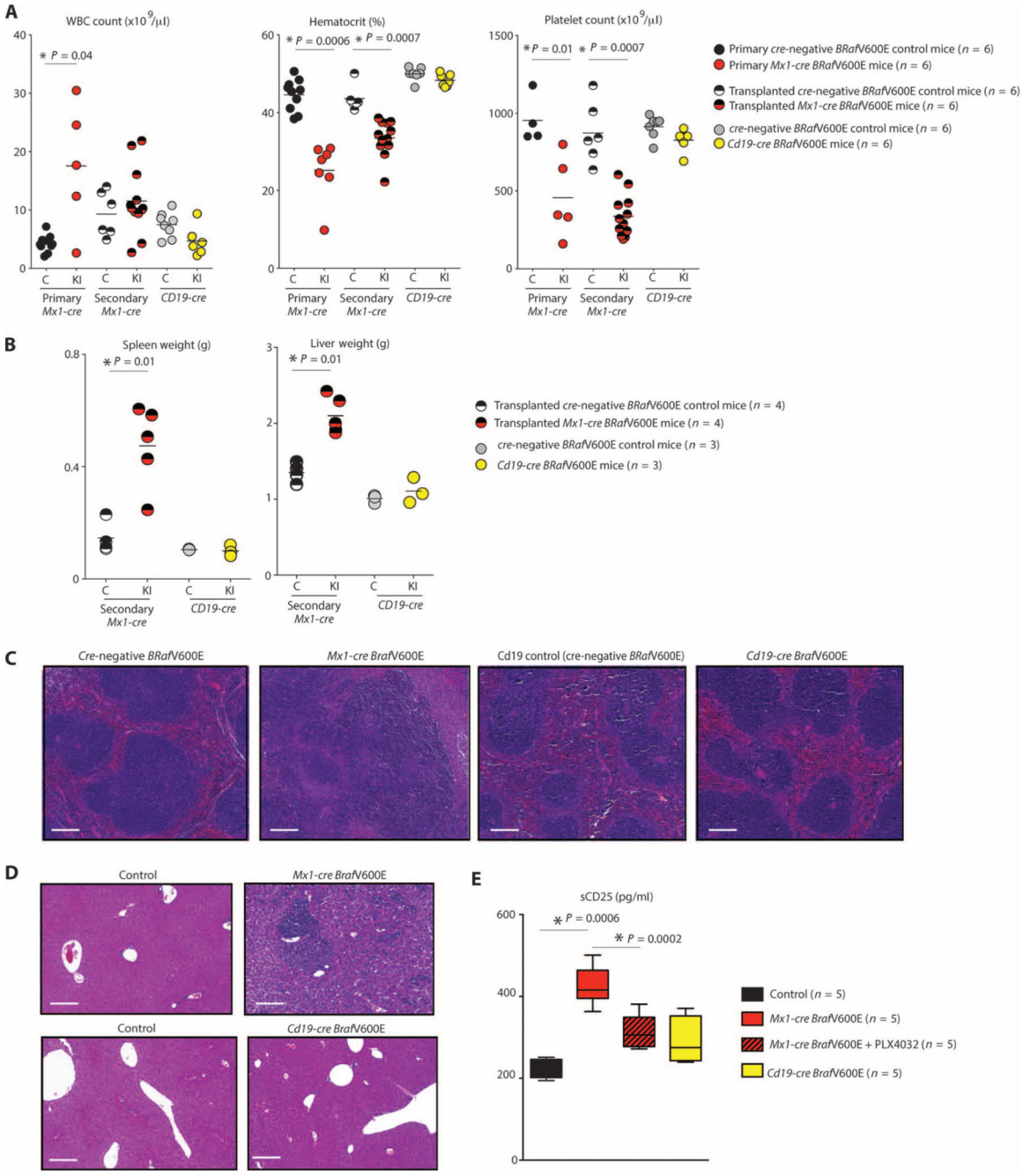

Fig. 3. Phenotypic analysis of mice with pan-hematopoietic versus B lineage–restricted expression of *BRaf*V600E

(**A**) White blood cell (WBC) count, hematocrit, and platelet count in 3-week-old primary *Mx1-cre BRaf*V600E mice, lethally irradiated CD45.2 recipient mice 6 weeks after transplantation with *Mx1-cre BRaf*V600E BM, and 3-week-old primary *Cd19-cre BRaf*V600E mice (C, Cre-negative *BRaf*V600E control; KI, Cre^{+} *BRaf*V600E knock-in; bar represents mean). (**B**) Weights of spleens and livers of lethally irradiated CD45.2 recipient mice 6 weeks after transplantation with *Mx1-cre BRaf*V600E BM versus 3-week-old *Cd19-*

*cre BRaf*V600E mice (bar represents mean). (**C** and **D**) Histological evaluation of spleens (C) and livers (D) from the same mice as in (B). Scale bars, 200 μm. (**E**) Quantification of serum concentrations of sCD25 in CD45.2 mice 6 weeks after transplantation with cre-negative *BRaf*V600E BM followed by 10 days of vehicle [5% dimethyl sulfoxide (DMSO), 1% methylcellulose] treatment ($n = 4$), *Mx1-cre BRaf*V600E BM followed by 10 days of vehicle (5% DMSO, 1% methylcellulose; $n = 5$), or PLX4720 treatment at 50 mg/kg twice daily ($n = 5$), or 12-week-old *Cd19-cre BRaf*V600E mice treated with vehicle ($n = 5$). sCD25 levels were significantly ($P = 0.001$) elevated in *Mx1-cre BRaf*V600E mice treated with vehicle compared with all other groups, and PLX4720 administration resulted in significant ($P = 0.002$) down-regulation of sCD25 (box and whiskers plot is shown with bottom and top of the box representing the first and third quartiles, and the band inside the box representing the median). *$P < 0.05$ (Mann-Whitney *U* test).

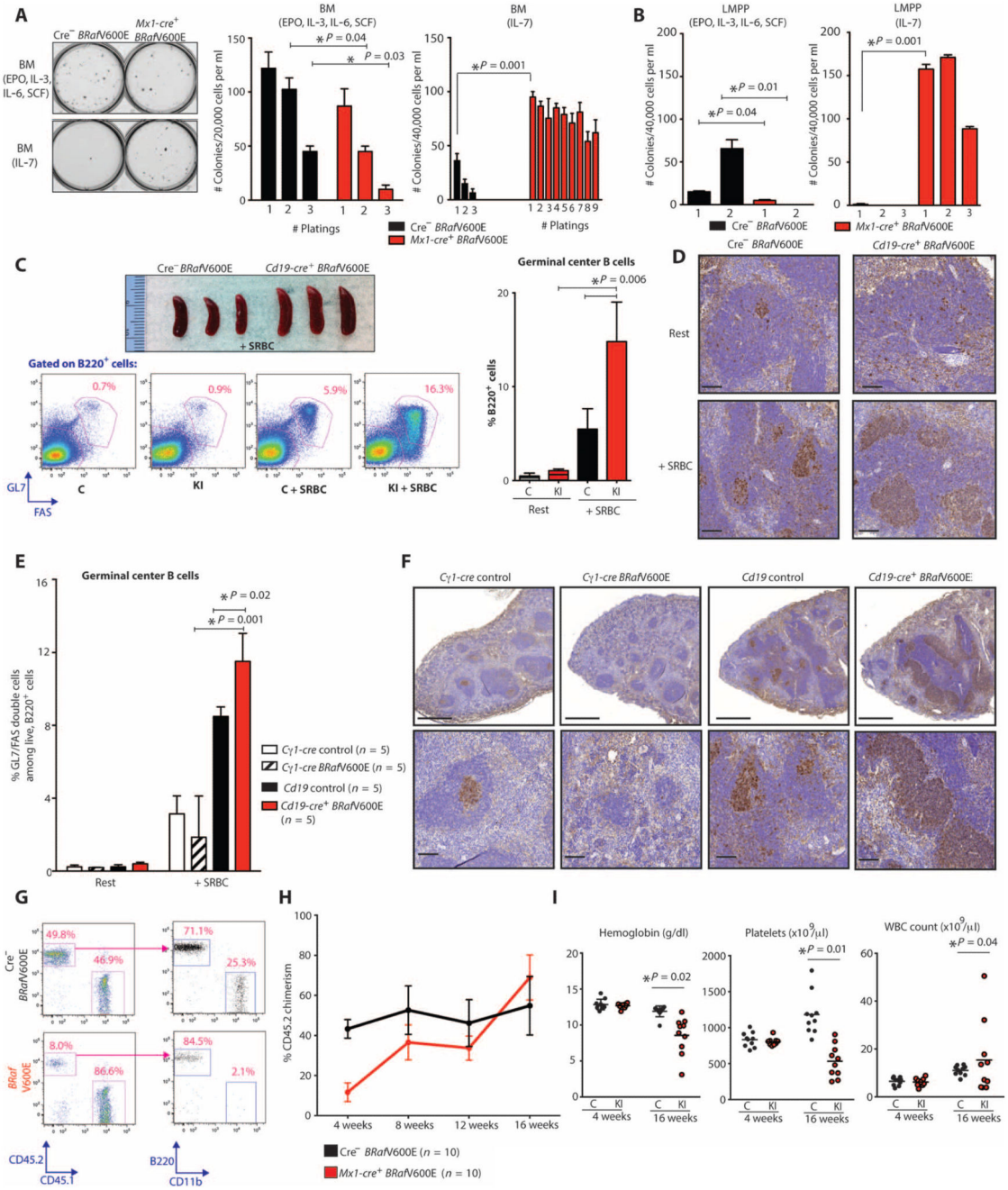

Fig. 4. Effect of *BRaf*V600E mutation on HSPC differentiation, self-renewal, and GC response to alloantigen

(**A** and **B**) Plating of whole BM (A) and sorted LMPP cells (B) in methylcellulose medium containing myeloid and erythroid cytokines (EPO, IL-3, IL-6, and SCF) or IL-7. *BRaf*V600E cells could be replated for >10 platings in the presence of IL-7. Photograph of initial plating shown on left. (**C** and **D**) GC response in *Cd19-cre BRaf*V600E (n = 5) and control mice (n = 5) 10 days after SRBC injection by gross photographs of mouse spleens (top), flow cytometric assessment (bottom and bar graph on right) (C), and immunohistochemistry for peanut agglutinin (PNA) (D). Scale bars, 100 μm. C, Cre-

negative *BRaf*V600E control; KI, *Cd19-cre BRaf*V600E. (**E** and **F**) GC response in *Cd19-cre BRaf*V600E and control mice alongside age-matched mice with GC-restricted *BRaf*V600E expression (*Cγ1-cre BRaf*V600E) by flow cytometry (E) and by PNA stain (F). Scale bars, 500 μm (top) and 100 μm (bottom). (**G** and **H**) Competitive transplantation of *Mx1-cre BRaf*V600E ($n = 10$ recipient mice) compared with *Cre*-negative *BRaf*V600E whole BM cells ($n = 10$ recipient mice) 4 weeks (G) and up to 16 weeks (H) after transplantation. (**I**) Mice transplanted with *BRaf*V600E hematopoietic cells in a competitive manner ($n = 10$ mice in control and $n = 10$ mice in knock-in group) developed anemia and thrombocytopenia concomitant with expansion of engrafted *BRaf*V600E HSPCs as shown in (H). Error bars represent means ± SD for (A) to (C), (E), and (H). Bar represents mean value in (I). $^*P < 0.05$ (Mann-Whitney *U* test).

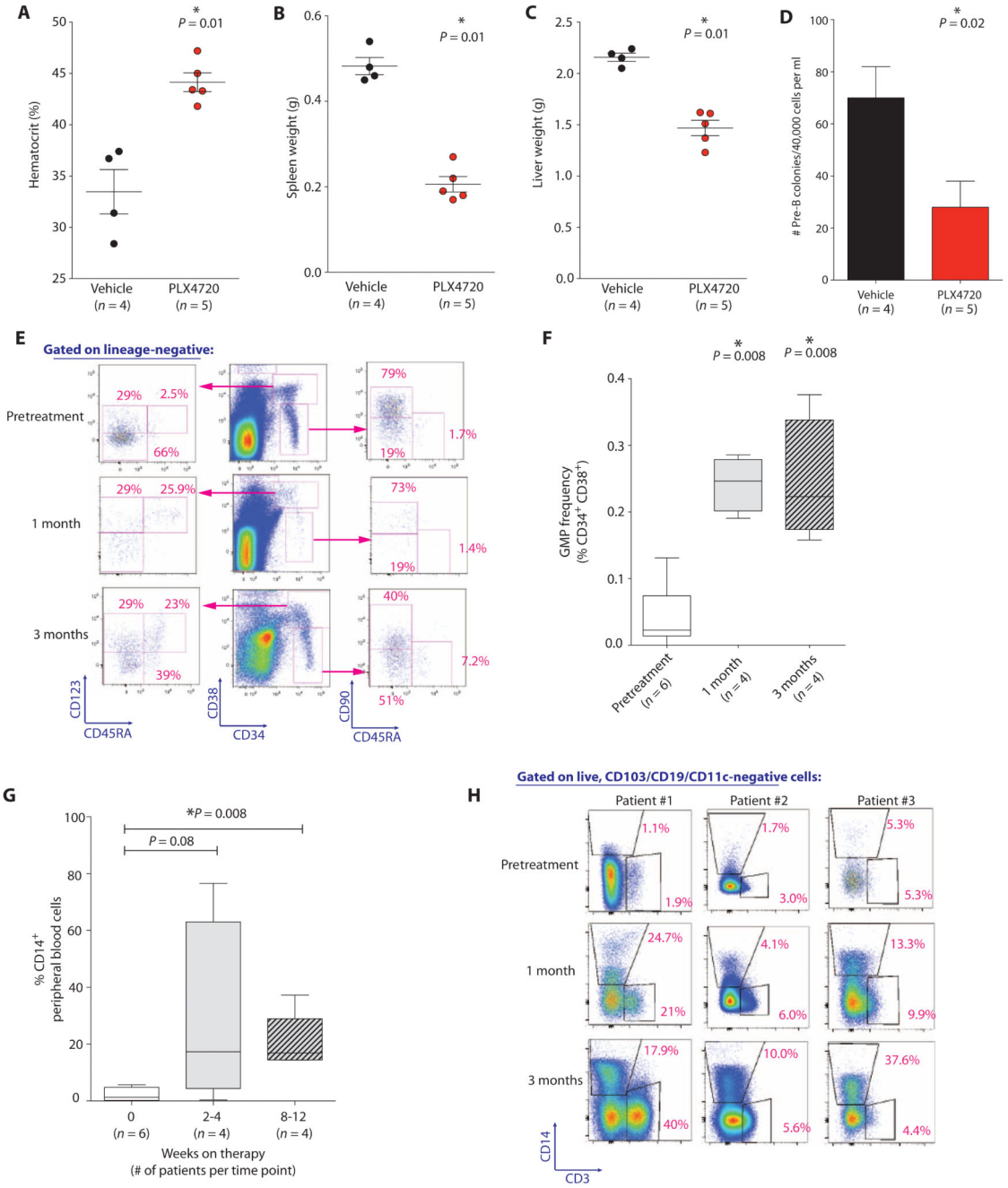

Fig. 5. Normalization of HSPC compartment and increased myeloid/erythroid output after BRAF inhibition

(**A** to **D**) Effect of 10 days of PLX4720 treatment (50 mg/kg orally twice daily) on hematocrit (A), spleen (B) and liver (C) weights, and ex vivo B cell colony formation (D) relative to vehicle (5% DMSO, 1% methylcellulose) treatment in *Mx1-cre BRaf*V600E mice. (**E**) Flow cytometric characterization of long-term HSC (LN $CD34^+$ $CD38^-$ $CD90^+$ $CD45RA^-$) and GMP frequencies (LN $CD19^-$ $CD10^-$ $CD34^+$ $CD38^+$ $CD123^+$ $CD45RA^+$) in serial BM aspirates from patients throughout vemurafenib therapy. (**F**) GMP frequencies

throughout vemurafenib therapy in *BRAF*V600E-mutant HCL patients (four to six patients per time point). BM aspirates were performed before treatment and at 1 and 3 months after vemurafenib as part of an ongoing phase 2 clinical trial of vemurafenib in HCL. (**G**) Percentage of $CD14^+$ cells among PB mononuclear cells in HCL patients throughout treatment (four to six patients per time point). (**H**) Analysis of $CD14^+$ and $CD3^+$ cells in PB of three patients throughout therapy. Error bars represent means ± SD in (A) to (D). (F and G) Box plots with band inside box representing median and ends of whiskers representing minimum and maximum values. $*P < 0.05$ (Mann-Whitney *U* test).